Optimum Design of Waveguide *E*-Plane Stub-Loaded Phase Shifters

JOACHIM DITTLOFF, FRITZ ARNDT, SENIOR MEMBER, IEEE, AND DIETRICH GRAUERHOLZ

***Abstract*—Novel broad-band low-insertion-loss *E*-plane stub-loaded rectangular waveguide phase shifters are designed with the method of field expansion into normalized eigenmodes, which includes higher order mode interaction between the step discontinuities. Computer-optimized three-stub prototypes of 90° differential phase shift with reference to an empty waveguide of appropriate length, designed for R140-band (12.4–18 GHz) and R320-band (26.5–40 GHz) waveguides, achieve typically ±0.5° phase shift deviation within about 20 percent bandwidth. For two-stub designs, the corresponding values are about +2.5°/−1° and 17 percent. Both designs achieve minimum return loss of 30 dB. The theory is verified by measurements at a compact R120-band (10–15 GHz) waveguide phase shifter design example milled from a solid block, showing measured insertion loss of about 0.1 dB and about +2.5°/−0.5° phase error between 10.7 and 12.7 GHz.**

I. Introduction

STUB LINE LOADING of transmission lines [1]–[7] is a well-known technique for building simple low-insertion-loss phase shifters for many circuit applications, such as switchable diode phase shifters realized in microstrip [4], [6], [7] or high-power coaxial line [5] configurations. This principle may advantageously be utilized for designing fixed waveguide phase shifters with broad-band nearly constant differential phase shift with reference to an empty waveguide over a desired frequency band. Fixed waveguide phase shifters are of considerable importance for composed components, e.g. for antenna beam-forming networks [8], where compact design and good overall performance depend on the requirements that the individual parts be sufficiently short and have appropriate electrical characteristics.

This paper presents a rigorous field theory method for designing simple compact broad-band rectangular waveguide phase shifters (Fig. 1). The advantages of the *E*-plane stub loading principle are such that convenient milling and spark eroding techniques from a solid block allow compact low-weight designs, that no severe problems may arise to meet the power specifications as no dielectric or ferrite materials are necessary, and that good VSWR and phase shift characteristics may be obtained by appropriate computer optimization of all relevant parameters. Moreover, the *E*-plane stub technique is highly compatible with printed *E*-plane components, [9], [10], and highly appropriate for millimeter-wave designs.

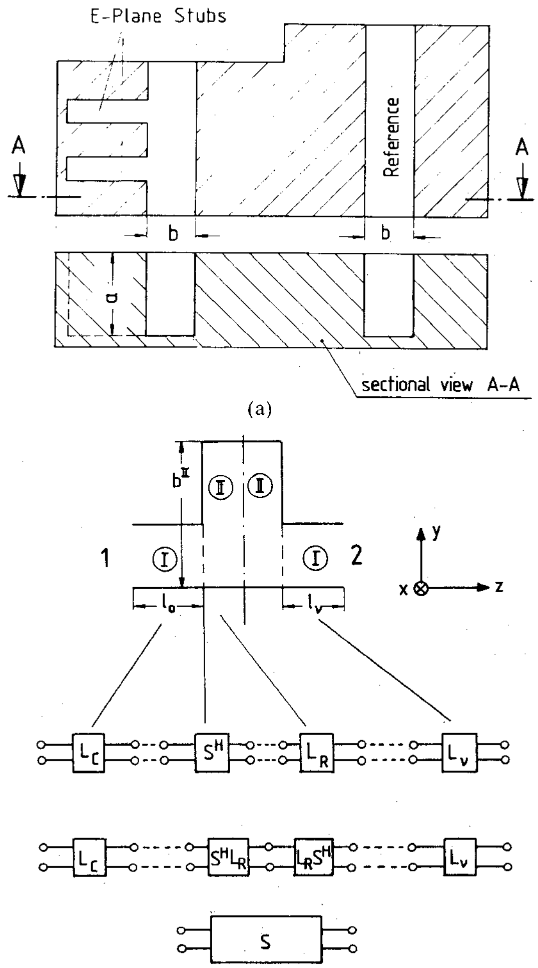

Fig. 1. *E*-plane stub loaded fixed phase shifter. (a) Waveguide with the stub sections, and the reference waveguide. (b) Sections for the field theory treatment.

Many analyses of *E*-plane stubs in rectangular waveguides have previously been reported, e.g. [11]–[15]. Moreover, the technique of iris-loaded waveguide phase shifters is well known [16]. These theories, however, utilize equivalent circuit representations of the discontinuities. As for dielectric or ferrite phase shifters [17], [18], the theory necessary for a rigorous treatment of the phase shift structure of Fig. 1 should take into account the higher order

Manuscript received May 21, 1987; revised August 26, 1987.
The authors are with the Microwave Department, University of Bremen, D-2800 Bremen 33, West Germany.
IEEE Log Number 8718866.

0018-9480/88/0300-0582$01.00

mode coupling effects at all discontinuities. The method for the computer optimization given in this paper, which is based on field expansion into normalized incident and scattered waves [19], meets these requirements and yields directly the overall scattering matrix along the stub-loaded structure. The theory is verified by measurements.

II. Theory

In solving for the modal S-matrix representation of the stub-loaded phase shifter (Fig. 1), we require only the field theory solution for a single waveguide discontinuity: change in waveguide height (Fig. 1(b)). Note that for the inverse discontinuity, from higher to lower waveguide, only the port designations of the related modal scattering matrix (i.e., from lower to higher waveguide) need to be interchanged. The total scattering matrix of the structure under consideration is formulated by suitable direct combination of the individual modal scattering matrices (S^H) by an iteration process already described [20], and by including appropriately the known scattering matrices (L) of a homogeneous waveguide section, for consideration of the distances between the individual discontinuities (Fig. 1(b)). This procedure preserves numerical accuracy, avoids instabilities, and requires no symmetry of modes [20].

As the modal scattering matrix of the discontinuity change in waveguide height has already been derived in [19], the theory is given here in abbreviated form only using the present notation. For details, the reader is referred to [19].

A TE_{10} wave incident in port 1 (Fig. 1(b)) excites longitudinal section TE^x_{1m} waves [21] at all step discontinuities. As in [19], therefore, for the homogeneous subregions $v = \mathrm{I}, \mathrm{II}$ (Fig. 1(b)) the fields [21]

$$\vec{E}^{(v)} = -j\omega\mu\nabla \times \vec{\Pi}^{(v)}_{hx} \qquad \vec{H}^{(v)} = \nabla \times \nabla \times \vec{\Pi}^{(v)}_{hx} \quad (1)$$

are derived from the x component of the magnetic Hertzian vector potential $\vec{\Pi}_h$, which is assumed to be a sum of suitable eigenmodes satisfying the vector Helmholtz equation and the boundary conditions:

$$\Pi^{(v)}_{hx} = \frac{2}{\sqrt{ab^{(v)}}} \cdot \frac{1}{\sqrt{k^2 - k_x^2}} \cdot \sin(k_x x) \cdot \sum_{n=0}^{N} \left[\frac{1}{\sqrt{Z^{(v)}_{Fn}}} \cdot \frac{1}{\beta^{(v)}_n} \frac{1}{\sqrt{1+\delta_{0n}}} \cdot \cos\left(k^{(v)}_{yn} y\right) \right] \cdot \left[A^{(v)}_n e^{-j\beta^{(v)}_n z} - B^{(v)}_n e^{+j\beta^{(v)}_n z} \right] \quad (2)$$

where

a = waveguide width,

$b^{(v)}$ = waveguide height in the subregion v,

$$k^2 = \omega^2\mu\epsilon, \quad k_x = \frac{\pi}{a},$$

$$Z^{(v)}_{Fn} = \frac{\omega\mu}{\beta^{(v)}_n},$$

$$k^{(v)}_y = \frac{n\pi}{b^{(v)}}, \quad \delta_{0n} = \text{Kronecker delta},$$

TABLE I
Optimized Two-Stub Phase Shifter Design Data for *Ku*-Band Waveguides ($a = 15.799$ mm, $b = a/2$) and *Ka*-Band Waveguides ($a = 7.122$ mm, $b = a/2$)

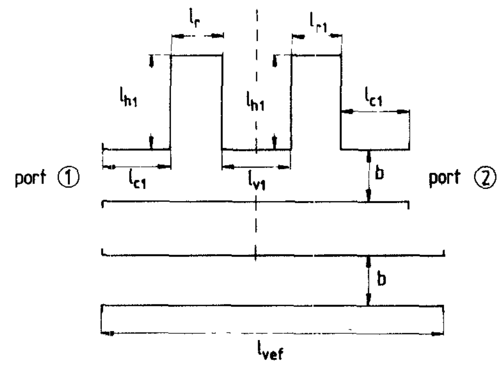

Dimensions (mm):

	Ku-Band	Ka-Band
l_{r1}	3.747	1.807
l_{h1}	12.627	6.089
l_{v1}	5 295	2.553
l_{c1}	5.703	2 750
l_{ref}	30 386	14 653

and

$$\beta^{(v)}_n = \begin{cases} \sqrt{\omega^2\mu\epsilon - \left(k_x^2 + k_y^{(v)2}\right)}, & \omega^2\mu\epsilon \geqslant k_x^2 + k_y^{(v)2} \\ -j\sqrt{\left(k_x^2 + k_y^{(v)2}\right) - \omega^2\mu\epsilon}, & \omega^2\mu\epsilon \leqslant k_x^2 + k_y^{(v)2}. \end{cases}$$

The eigenmodes in (2) with the still-unknown amplitude coefficients A_n and B_n are suitably normalized, so that the power carried by a given wave is 1 W for a wave amplitude coefficient of $1\sqrt{W}$ [21].

By matching the tangential field components at the common interface between subregions I and II (Fig. 1(b)), and utilizing the orthogonal property of the modes [21], the amplitude coefficients of (2) are related to each other in the form of the desired modal scattering matrix (S^H) of the discontinuity change in waveguide height:

$$\begin{pmatrix} (B^{\mathrm{I}}) \\ (A^{\mathrm{II}}) \end{pmatrix} = (S^H) \begin{pmatrix} (A^{\mathrm{I}}) \\ (B^{\mathrm{II}}) \end{pmatrix}. \quad (3)$$

For completeness, the matrix elements are given in the Appendix.

For computer optimization, the expansion into ten eigenmodes at each step discontinuity and four eigenmodes along each intermediate homogeneous waveguide section has turned out to yield sufficient asymptotic behavior of the coefficients of the total scattering matrix of the structure, calculated iteratively according to [20]. The final design data are provided by expansion into 20 eigenmodes.

The computer-aided design is carried out by an optimizing program [19] applying the evolution strategy method, i.e., a modified direct search method [22], which varies the

TABLE II
OPTIMIZED THREE-STUB PHASE SHIFTER DESIGN DATA FOR *Ku*- AND *Ka*-BAND WAVEGUIDES

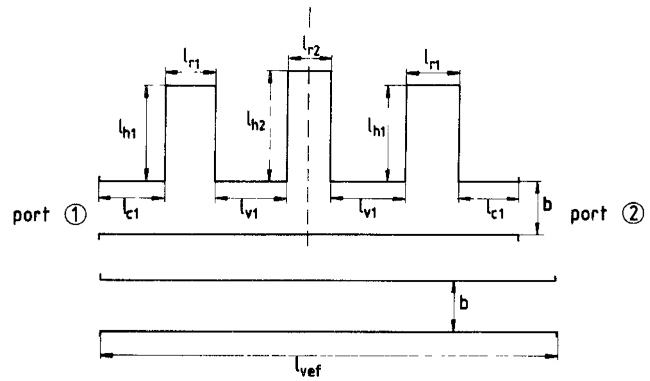

Dimensions (mm)

	Ku-Band	Ka-Band
l_{r1}	2.521	1.093
l_{r2}	3.422	1570
l_{h1}	13.038	5 974
l_{h2}	12 865	5 888
l_{c1}	5.836	2.262
l_{v1}	4 172	1 935
l_{ref}	34 705	15.003

input parameters statistically until the desired phase shifter characteristics for a given bandwidth are obtained. An error function $F(\bar{x})$ to be minimized is defined

$$F(\bar{x}) = \sum_{i=1}^{I} \left\{ \left[S_{11}(f_i)/S_{11D} \right]^2 + \left[\left| \mathrm{arc}\left(S_{21}(f_i)\right) - \mathrm{arc}\left(S_{21\,\mathrm{ref}}(f_i)\right) \right| - \Delta\varphi_D \right]^2 \right\} \overset{!}{=} \mathrm{Min} \tag{4}$$

where I is the number of frequency sample points f_i; S_{11D} and $\Delta\varphi_D$ are the desired input reflection coefficient and differential phase shift, respectively; S_{11} and S_{21} are the calculated scattering coefficients of the phase shifter (Fig. 1) at the frequency f_i; and $S_{21\,\mathrm{ref}}$ is the scattering coefficient of the related homogeneous reference waveguide section (Fig. 1). For desired waveguide housing dimensions a, b, and number of stub sections, the parameters to be optimized (Tables I, II) are the dimensions of the stub sections, the lengths of the intermediate waveguide sections, and the length of the reference waveguide section. The number of frequency sample points was chosen to be ten.

III. RESULTS

Optimized design data for fixed waveguide phase shifters with two and three stubs, respectively, are given in Tables I and II, for *Ku*-band waveguides (12.4–18 GHz, $a = 15.799$ mm, $b = a/2$) and *Ka*-band waveguides (26–40 GHz, $a = 7.112$ mm, $b = a/2$). Fig. 2 shows the input reflection coefficient as well as the differential phase shift of the *Ka*-band two-stub example as a function of frequency. A minimum return loss of 30 dB is achieved within about 15 percent bandwidth; the phase shift deviation from the desired 90° is $+2.5°/-1°$.

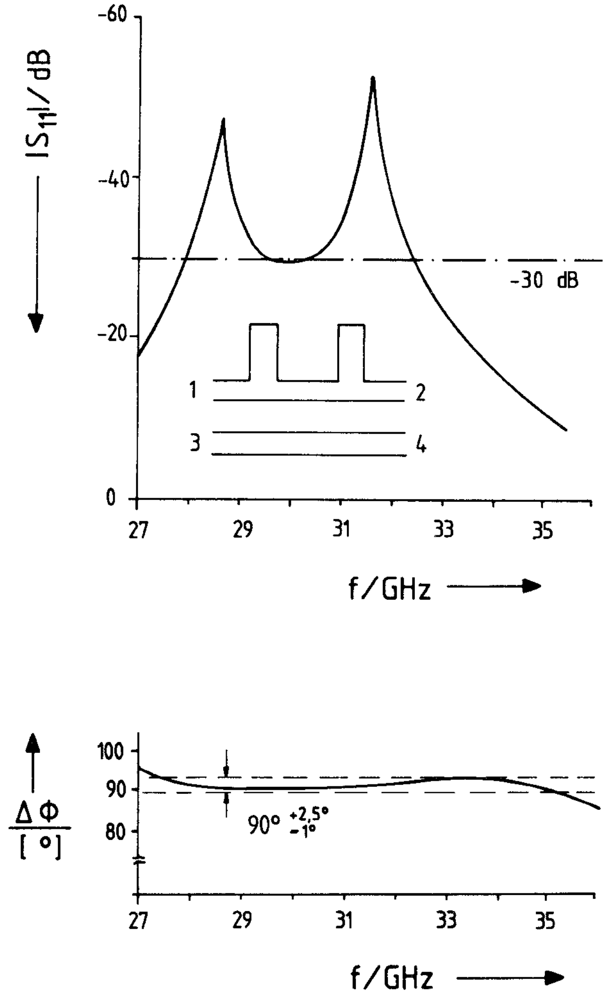

Fig. 2. Input reflection coefficient in decibels and differential phase shift versus frequency of the *Ka*-band two-stub phase shifter.

The three-stub design examples (Figs. 3 and 4) provide a differential phase shift of $90° \pm 0.5°$, together with minimum 30 dB return loss, within about 20 percent bandwidth.

Fig. 5(a) shows the photograph of an *E*-plane fixed phase shifter example for R120 input and output waveguides ($a = 19.05$ mm, $b = a/2$), which was milled from a solid block to produce waveguide channels of identical a-dimension milling depth, and was spark eroded to size in the more critical areas of corners and steps. The component has been fabricated in the antenna department of MBB/Erno, Munich, W. Germany, by utilizing a computer-aided milling technique. The realized component shows a measured insertion loss of only about 0.1 dB, and a phase error of about $+2.5°/-1°$, between 10.7 and 12.7 GHz. The theoretical predicted values (Fig. 5(b)) demonstrate excellent agreement with the measured results.

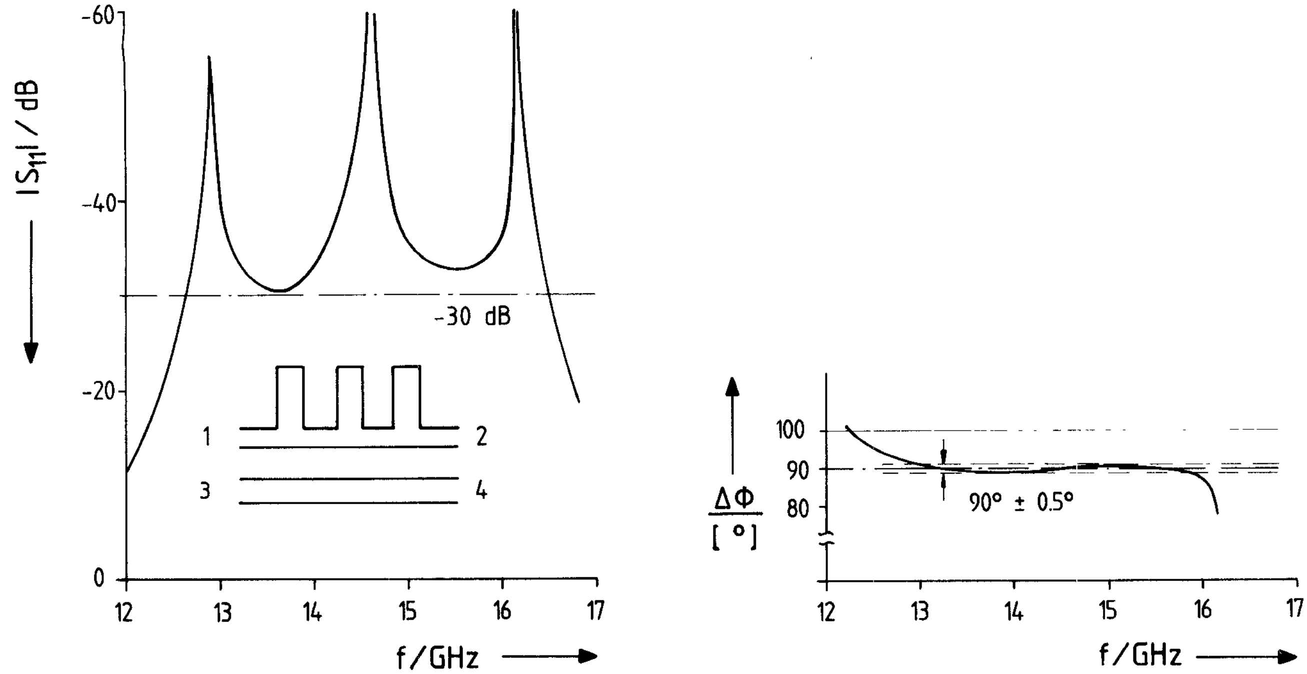

Fig. 3. Input reflection coefficient in decibels and differential phase shift versus frequency of the *Ku*-band three-stub phase shifter.

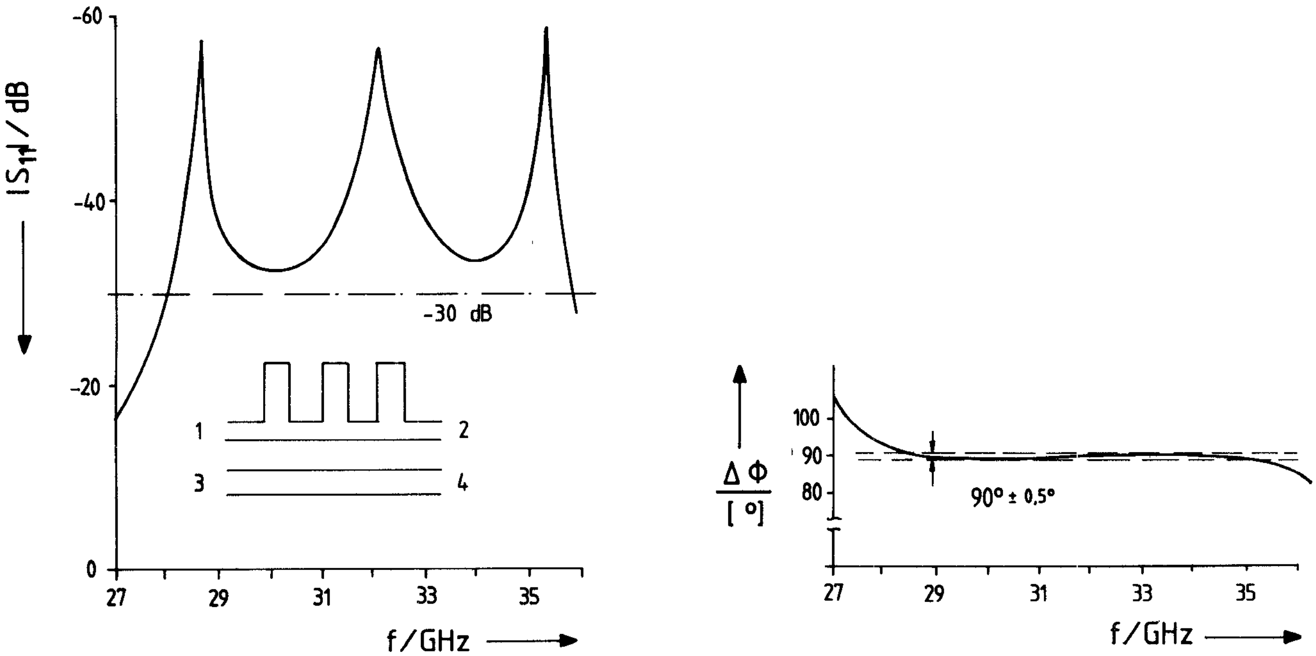

Fig. 4. Input reflection coefficient in decibels and differential phase shift versus frequency of the *Ka*-band three-stub phase shifter.

IV. Conclusions

Novel broad-band low-insertion-loss *E*-plane stub-loaded rectangular waveguide phase shifters are designed which lead to compact structures highly appropriate for composed components, such as antenna-beam forming networks, up to millimeter waves. The method of computer optimization, which is based on field expansion into normalized incident and scattered waves, takes the higher order mode coupling effects rigorously into account, and yields directly the overall scattering matrix. The good agreement between theory and measurements shows that the design theory presented allows the direct high-precision manufacturing of compact fixed waveguide phase shifters without the necessity for additional trial-and-error adjustment methods.

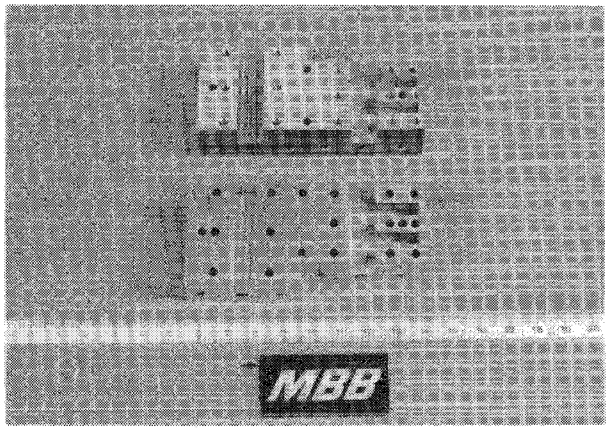

(a)

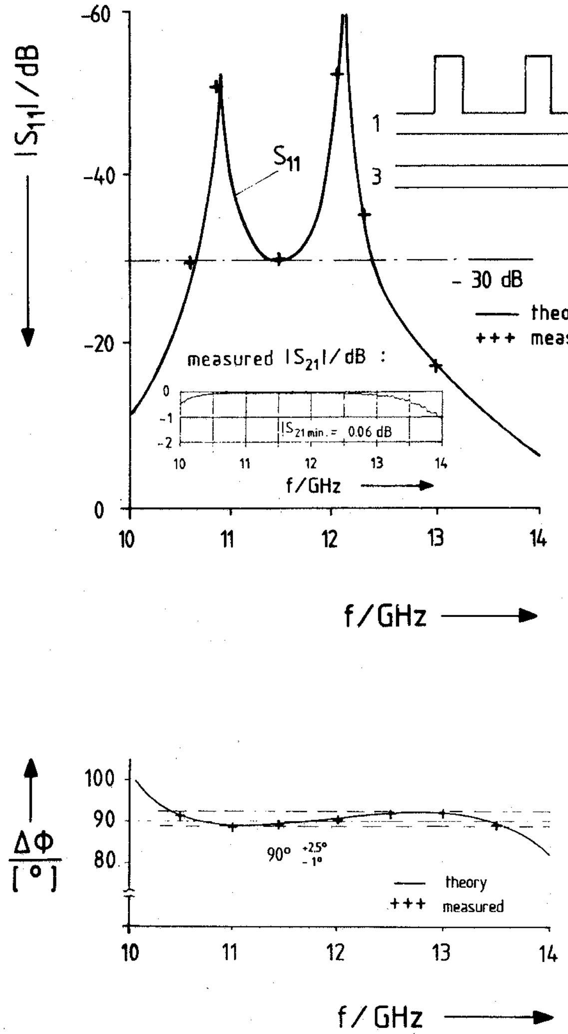

(b)

Fig. 5. Realized two-stub phase shifter for R120-band waveguide (10–15 GHz, $a = 19.05$ mm, $b = a/2$). (a) Photograph of the phase shifter milled from a solid block (by MBB) to produce waveguide channels of identical a-dimension (photograph courtesy of Antenna Dpt. MBB/Erno, Munich, W. Germany). (b) Input reflection coefficient in decibels and differential phase shift versus frequency (—theory, + + + measured).

Appendix

Submatrices of (3):

$$\begin{aligned}(S_{11}^H) = {} & \Big[(\sqrt{Y_m})(1/\beta_m)\big[(K_{1nm})(\sqrt{Y_m})\big]^{-1}(\sqrt{Y_n}) \\ & + (K_{2mn})(1/\beta_n)(\sqrt{Y_n})\Big]^{-1} \\ & * \Big[-(\sqrt{Y_m})(1/\beta_m)\big[(K_{1nm})(\sqrt{Y_m})\big]^{-1}(\sqrt{Y_n}) \\ & + (K_{2mn})(1/\beta_n)(\sqrt{Y_n})\Big] \end{aligned} \tag{A1}$$

$$\begin{aligned}(S_{12}^H) = {} & 2\Big[(\sqrt{Y_m})(1/\beta_m)\big[(K_{1nm})(\sqrt{Y_m})\big]^{-1}(\sqrt{Y_n}) \\ & + (K_{2mn})(1/\beta_n)(\sqrt{Y_n})\Big]^{-1}(\sqrt{Y_m})(1/\beta_m) \end{aligned} \tag{A2}$$

$$\begin{aligned}(S_{21}^H) = {} & 2\Big[(K_{1nm})(\sqrt{Y_m}) + (\sqrt{Y_n})\big[(K_{2mn})(1/\beta_n)(\sqrt{Y_n})\big]^{-1} \\ & * (\sqrt{Y_m})(1/\beta_m)\Big]^{-1}(\sqrt{Y_n}) \end{aligned} \tag{A3}$$

$$\begin{aligned}(S_{22}^H) = {} & \Big[(K_{1nm})(\sqrt{Y_m}) + (\sqrt{Y_n})\big[(K_{2mn})(1/\beta_n)(\sqrt{Y_n})\big]^{-1} \\ & * (\sqrt{Y_m})(1/\beta_m)\Big]^{-1} \\ & * \Big[-(K_{1nm})(\sqrt{Y_m}) + (\sqrt{Y_n})\big[(K_{2mn})(1/\beta_n)(\sqrt{Y_n})\big]^{-1} \\ & * (\sqrt{Y_m})(1/\beta_m)\Big]. \end{aligned} \tag{A4}$$

Coefficients of the Coupling Matrices $(K_1), (K_2)$:

$$\begin{aligned} K_{1nm} = {} & \frac{1}{\sqrt{1+\delta_{0m}}} \cdot \frac{1}{\sqrt{1+\delta_{0n}}} \cdot \frac{2}{\sqrt{b \cdot b^{\mathrm{II}}}} \\ & \cdot \int_0^b \cos\left[\frac{m\pi}{b}(y)\right] \cdot \cos\left[\frac{n\pi}{b^{\mathrm{II}}}(y)\right] dy \\ (K_{2mn}) = {} & (K_{1mn})' \quad ('= \text{transposed}). \end{aligned} \tag{A5}$$

Elements of the Diagonal Matrices $(\sqrt{Y_m})$, $(\sqrt{Y_n})$, $(1/\beta_m)$, $(1/\beta_n)$:

$$\begin{aligned} \sqrt{Y_m} = \frac{1}{\sqrt{Z_{Fm}^{\mathrm{II}}}} \qquad & \sqrt{Y_n} = \frac{1}{\sqrt{Z_{Fn}^{\mathrm{I}}}} \\ (1/\beta_m)_m = 1/\beta_m^{\mathrm{II}} \qquad & (1/\beta_n)_n = 1/\beta_n^{\mathrm{I}}. \end{aligned} \tag{A6}$$

Acknowledgment

The authors gratefully acknowledge the permission for presentation of the photograph of the phase shifter and of the measured values in Fig. 5 by Dr. Fasold and Dipl.-Ing. Schröder of the Antenna Department of MBB/Erno, Munich, W. Germany, where the component has been fabricated and measured.

References

[1] H. N. Dawirs and W. G. Swarner, "A very fast voltage controlled microwave phase shifter," *Microwave J.*, vol. 5, pp. 99–106, June 1962.

[2] J. F. White, "High power p-i-n diode controlled, microwave transmission phase shifter," *IEEE Trans. Microwave Theory Tech.*, vol. MTT-13, pp. 233–242, Mar. 1965.

[3] R. V. Garver, "Broad-band diode phase shifters," *IEEE Trans. Microwave Theory Tech.*, vol. MTT-20, pp. 314–323, May 1972.
[4] J. F. White, "Diode phase shifters for array antennas," *IEEE Trans. Microwave Theory Tech.*, vol. MTT-22, pp. 658–674, June 1974.
[5] J. F. White, "Origins of high-power diode switching," *IEEE Trans. Microwave Theory Tech.*, vol. MTT-32, pp. 1105–1117, Sept. 1984.
[6] I. J. Bahl and K. C. Gupta, "Design of loaded-line p-i-n diode phase shifter circuits," *IEEE Trans. Microwave Theory Tech.*, vol. MTT-28, pp. 219–224, Mar. 1980.
[7] H. A. Atwater, "Circuit design of the loaded-line phase shifter," *IEEE Trans. Microwave Theory Tech.*, vol. MTT-33, pp. 626–634, July 1985.
[8] R. Levy, "A high-power *X*-band Butler matrix," *Microwave J.*, vol. 27, pp. 135–141, Apr. 1984.
[9] P. J. Meier, "Integrated finline: The second decade," *Microwave J.*, vol. 28, no. 11, pp. 31–54, Nov. 1985; also no. 12, pp. 30–48, Dec. 1985.
[10] K. Solbach, "The status of printed millimeter-wave *E*-plane circuits," *IEEE Trans. Microwave Theory Tech.*, vol MTT-31, pp. 107–121, Feb. 1983.
[11] N. Marcuvitz, *Waveguide Handbook*. New York: McGraw-Hill, 1951, ch. 6, 7.
[12] G. L. Matthaei, L. Young, and E. M. T. Jones, *Microwave Filters, Impedance-Matching Networks, and Coupling Structures*. New York: McGraw-Hill, 1964, ch. 12, 13.
[13] R. Levy, "Analysis of practical branch-guide directional couplers," *IEEE Trans. Microwave Theory Tech.*, vol. MTT-17, pp. 289–290, May 1969.
[14] E. Kühn, "Microwave band-stop filters using quarter-wave-coupled open *E*-plane stubs in rectangular waveguide," *Arch. Elek. Übertragung.*, vol. 29, pp. 138–143, Mar. 1975.
[15] R. Geißler, and Z. Chahabadi, "Hohlleiter-Filter für das *R*-band (26.5–40 GHz)," *Arch. Elek. Übertragung.*, vol. 33, pp. 46–48, Jan. 1979.
[16] A. J. Simmons, "Phase shift by periodic loading of waveguide and its application to broad-band circular polarization," *IEEE Trans. Microwave Theory Tech.*, vol. MTT-3, pp. 18–21, Dec. 1955.
[17] F. Arndt, A. Frye, M. Wellnitz, and D. Wirsing, "Double dielectric-slab-filled waveguide phase shifter," *IEEE Trans. Microwave Theory Tech.*, vol. MTT-33, pp. 373–381, May 1985.
[18] J. Uher, F. Arndt, and J. Bornemann, "Field theory design of ferrite-loaded waveguide nonreciprocal phase shifters with multisection ferrite on dielectric slab impedance transformers," *IEEE Trans. Microwave Theory Tech.*, vol. MTT-35, pp. 552–560, June 1987.
[19] F. Arndt, B. Koch, H.-J. Orlock, and N. Schröder, "Field theory design of rectangular waveguide broadwall metal insert slot couplers for millimeter-wave applications," *IEEE Trans. Microwave Theory Tech.*, vol. MTT-33, pp. 95–104, Feb. 1985.
[20] H. Patzelt and F. Arndt, "Double-plane steps in rectangular waveguides and their applications for transformers, irises, and filters," *IEEE Trans. Microwave Theory Tech.*, vol. MTT-30, pp. 771–776, May 1982.
[21] R. E. Collin, *Field Theory of Guided Waves*. New York: McGraw-Hill, 1960, pp. 338–348, 171–179, 85–87.
[22] H. Schmiedel, "Anwendung der Evolutionsoptimierung bei Mikrowellenschaltungen," *Frequenz*, vol. 35, pp. 306–310, Nov. 1981.

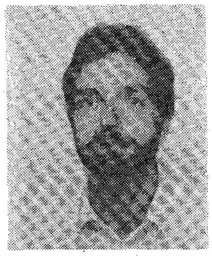

Joachim Dittloff was born in Rotenburg (Wümme), West Germany, on January 6, 1959. In 1984, he received the Dipl.-Ing. degree from the University of Bremen, West Germany, for research in microwave applications (power dividers).

Since then he has been with Prof. F. Arndt at the Microwave Department of the University of Bremen. His work is concentrating on rectangular waveguide components (phase shifters, power dividers, multiplexing structures and filters).

Fritz Arndt (SM'83) was born in Konstanz, Germany, on April 30, 1938. He received the Dipl.-Ing., Dr. Ing., and Habilitation degrees from the Technical University of Darmstadt, Germany, in 1963, 1968, and 1972, respectively.

From 1963 to 1973, he worked on directional couplers and microstrip techniques at the Technical University of Darmstadt. Since 1972, he has been a Professor and Head of the Microwave Department of the University of Bremen, Germany. His research activities are in the area of the solution of field problems of waveguide, finline, and optical waveguide structures, of antenna design, and of scattering structures.

Dr. Arndt is a member of the VDE and NTG (Germany). He received the NTG award in 1970, the A. F. Bulgin Award (together with three coauthors) from the Institution of Radio and Electronic Engineering in 1983, and the best paper award of the Antenna Conference JINA 1986 (France).

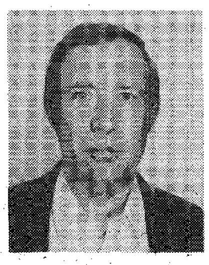

Dietrich Grauerholz was born in Krems II, Germany, on September 22, 1945. He received the Dipl.-Ing. degree in 1971.

From 1971 to 1973 he worked in the High-Frequency Laboratory of Electro-Spezial (Philips). In 1973 he joined the Microwave Department of the University of Bremen, Bremen, Germany, where he has been engaged in the research and development of microstrip circuits, finline structures, and microwave measurements.